Peri-ictal hypoxemia during temporal lobe seizures: A SEEG study

Julien Jung, Romain Bouet, Hélène Catenoix, Alexandra Montavont, Jean Isnard, Sébastien Boulogne, Marc Guénot, Philippe Ryvlin, Sylvain Rheims

Received: 11 February 2022 | Revised: 4 May 2022 | Accepted: 25 May 2022

DOI: 10.1002/hbm.25975

RESEARCH ARTICLE

WILEY

Peri-ictal hypoxemia during temporal lobe seizures: A SEEG study

Julien Jung[1,2] | Romain Bouet[2] | Hélène Catenoix[1,2] | Alexandra Montavont[1,2] | Jean Isnard[1,2] | Sébastien Boulogne[1,2] | Marc Guénot[3,2] | Philippe Ryvlin[4] | Sylvain Rheims[1,2]

[1]Department of Functional Neurology and Epileptology, Hospices Civils de Lyon and University of Lyon, Lyon, France

[2]Lyon Neuroscience Research Center, INSERM U1028/CNRS UMR 5292 and Lyon 1 University, Lyon, France

[3]Department of Functional Neurosurgery, Hospices Civils de Lyon and University of Lyon, Lyon, France

[4]Department of Clinical Neurosciences, Vaudois University Hospital Center, Lausanne, Switzerland

Correspondence
Julien Jung, Department of Functional Neurology and Epileptology, 59 Boulevard Pinel, 69677 Bron Cedex, France.
Email: julien.jung@chu-lyon.fr

Funding information
Ministry Of Health

Abstract

Focal seizures originating from the temporal lobe are commonly associated with peri-ictal hypoxemia (PIH). During the course of temporal lobe seizures, epileptic discharges often not only spread within various parts of the temporal lobe but also possibly insula and frontal lobe. The link between spatial propagation of the seizure discharges and PIH is still unclear. The present study investigates the involvement of several brain structures including medial temporal structures, temporal pole, anterior insula, and frontal cortex in the occurrence of PIH. Using quantitative indices obtained during SEEG (stereoencephalography) recordings in 38 patients, we evaluated the epileptogenicity, the spatial propagation, and functional connectivity between those structures during seizures leading to PIH. Multivariate statistical analyses of SEEG quantitative indices showed that temporal lobe seizures leading to PIH are characterized by a strong involvement of amygdala and anterior insula during seizure propagation and a more widespread involvement of medial temporal lobe structures, lateral temporal lobe, temporal pole, and anterior cingulate at the end of the seizures. On the contrary, seizure-onset zone was not associated with PIH occurrence. During seizure propagation, anterior insula, temporal pole, and temporal lateral neocortex activities were correlated with intensity of PIH. Lastly, PIH occurrence was also related to a widespread increase of synchrony between those structures. Those results suggest that PIH occurrence during temporal lobe seizures may be related to the activation of a widespread network of cortical structures, among which amygdala and anterior insula are key nodes.

KEYWORDS
connectivity, hypoxemia, networks, stereoelectroencephalography, temporal lobe seizures

1 | INTRODUCTION

Peri-ictal hypoxemia is frequently observed during focal seizures, especially in those of temporal lobe origin (Lacuey et al., 2018; Tio et al., 2020; Vilella et al., 2019). The seminal study of Bateman analyzed 304 seizures and showed that desaturation below 90% was observed in at least one seizure in 64% of patients and 34% of all focal seizures without secondary generalization were associated with

hypoxemia (Bateman et al., 2008). However, the authors concluded that desaturations below 90% were five times more frequent in temporal lobe seizures than in extratemporal lobe seizures. During temporal lobe seizures, epileptic discharges often propagate across several brain regions, including medial and neocortical regions, but also distant cortical areas (Bartolomei et al., 2001; Maillard et al., 2004). Like other ictal symptoms, PIH occurrence may be related to the disruption of functional brain networks during seizure propagation. However, the localization value of PIH for assessing preferential seizure-propagation pathways is not established.

PIH is primarily related to peri-ictal central apnea (Bateman et al., 2008; Lacuey et al., 2018). Therefore, studying seizure networks activated during PIH may also contribute to clarify the pathophysiology of respiratory dysfunction that can lead to fatal post-ictal central apnea (Ryvlin et al., 2013).

Several studies suggested that ictal and/or post-ictal respiratory dysfunction occurring during focal seizures might be related to the involvement of cortical regions involved in the regulation of respiration (Lacuey et al., 2017; Lacuey, Hampson, et al., 2019; Nobis et al., 2019; Park et al., 2020). Direct electrical stimulation of the mesial temporal structures, especially the amygdala, can reliably induce transient apnea and hypoxemia (Dlouhy et al., 2015; Lacuey et al., 2017; Lacuey, Hampson, et al., 2019). Neuroimaging studies have shown that several structures, including medial temporal lobe, anterior insula, medial temporal pole, and anterior cingulate are involved in the cortical control of breathing (Evans, 2010). Electrical stimulations of those regions may also lead to transient hypoxemia. (Kaada & Jasper, 1952a; Loizon et al., 2020; Ochoa-Urrea et al., 2021) Taken together, those studies suggest that those structures may be considered as potential drivers of PIH generation. However, direct evidence of their involvement and interaction during seizures associated with PIH is lacking.

To tackle these issues, we evaluated whether temporal lobe seizures associated with PIH are characterized by a preferential propagation to several regions involved in respiratory control including amygdala, hippocampus, anterior insula, temporal pole, and frontal cortex in patients undergoing SEEG (stereoelectroencephalography) recordings. We also postulated that PIH occurrence is associated with stronger functional connectivity between those structures.

2 | MATERIALS AND METHODS

2.1 | Patients

Patients were identified among those who participated **in** the REPO$_2$MSE study at Department of Functional Neurology, Hospices Civils de Lyon, Lyon, France, between January 01, 2010 and October 31, 2018. The REPO$_2$MSE study is a multicenter prospective study whose primary objective is to individualize risk factors of SUDEP in patients suffering from drug-resistant focal epilepsy (*NCT02572297*).

For the present study, the patients were selected according to the following criteria: (i) Noninvasive presurgical assessment (including scalp video-EEG monitoring, brain multimodal MRI, and interictal FDG PET) suggesting temporal lobe epilepsy but requiring mandatory video-SEEG recordings for surgical decisions; (ii) long-term intracerebral EEG recordings using SEEG performed at the Department of Functional Neurology and Epileptology, Hospices Civils de Lyon, Lyon, France; (iii) valid pulse oximetry (SpO_2) measurement at seizure onset and during the course of the seizure in ≥1 recorded focal seizure (FS); focal to bilateral tonic–clonic seizures were excluded.

Overall, 38 patients were included in the present study. According to inclusion criteria, all of them suffered from drug-resistant focal epilepsy with ictal clinical features and scalp EEG suggesting predominant involvement of temporal lobe structures but with atypical features for medial temporal lobe syndrome including i) atypical ictal symptoms (symptoms suggesting propagation to neocortical regions or insula or perisylvian cortex) or ii) unusual ictal EEG pattern iii) absence of hippocampal sclerosis. The objective of SEEG in these patients was therefore to discriminate a mesial temporal epileptogenic zone from a temporal neocortical or a temporal plus epilepsy (Barba et al., 2016).

For 36 patients, recorded seizures led systematically either to PIH or no-PIH: a single representative seizure was extracted. For two patients, two distinct seizures were extracted since one led to PIH and one was not associated with PIH. Detailed clinical characteristics of the 38 patients are shown in Table S3.

2.2 | Video-SEEG recordings

All patients were chronically implanted with 12 to 15 stereotactic multilead depth electrodes for 1 to 2 weeks (DIXI Medical Instrument) targeting various brain structures within medial temporal, lateral temporal lobe, insula, and frontal lobe.

T1-weighted MRI was acquired after surgery. Exact contact locations were manually determined from the position of the corresponding artifact on the postoperative MRI.

SEEG data were recorded continuously using a 258- channels video-EEG monitoring system (Micromed; sampling rate, 256 Hz) during interictal periods and seizures. The reference electrode was a contact in the cerebral white matter.

2.3 | SEEG signals analysis

All SEEG signals were re-referenced using bipolar montages between neighboring contacts of the same electrode. For each patient, the SEEG signals for at least one seizure were extracted.

2.3.1 | Regions of interest

For each patient, the SEEG bipolar signal from selected brain regions of interest (ROI) was extracted. Those regions of interest were: anterior hippocampus, amygdala, anterior cingulate gyrus (BA24), anterior

insula (short gyri of the insula – BA13), lateral temporal cortex (BA21), temporal pole (BA38), frontal lateral region including frontal operculum (BA44, BA45, or BA46), and orbito frontal cortex (BA47 and BA11). For each ROI, a single bipole was extracted per patient based on visual identification on postimplantation MRI. When several dipoles sampled a given region, the dipole with the most clear ictal EEG changes was chosen. For 16 patients, an implantation of both temporal lobes was performed with a majority of SEEG electrodes targeting one hemisphere and one or two contralateral temporal lobe electrodes. Tables S1 and S2 show a summary of implanted regions of interest across patients and the details of implanted structures for each patient.

2.3.2 | Temporal segmentation of ictal SEEG data

The course of the seizure was segmented into four periods: baseline, seizure onset, seizure propagation, and seizure end (Figure 1). The baseline period was a time period of 20 s at least 1 min before seizure onset. Seizure onset was defined as the 10 s following the seizure start determined with Epileptogenicity Index, a quantitative index providing a detection time for each brain structure involved in the generation of a rapid discharge at seizure onset (Bartolomei et al., 2008). Seizure propagation was defined as a time period of 10 s corresponding to a spatial spread of the discharge outside of the defined seizure-onset zone with a clear change of ictal SEEG patterns (from low voltage fast activity above 20 Hz to slower activity with rhythmic spikes). The time position of the seizure propagation relative to seizure onset was adapted for each but corresponded roughly at the middle part of the seizure (onset of seizure propagation between 30% and 70% of the whole seizure duration). Seizure end were the 10 s preceding the termination of the seizures.

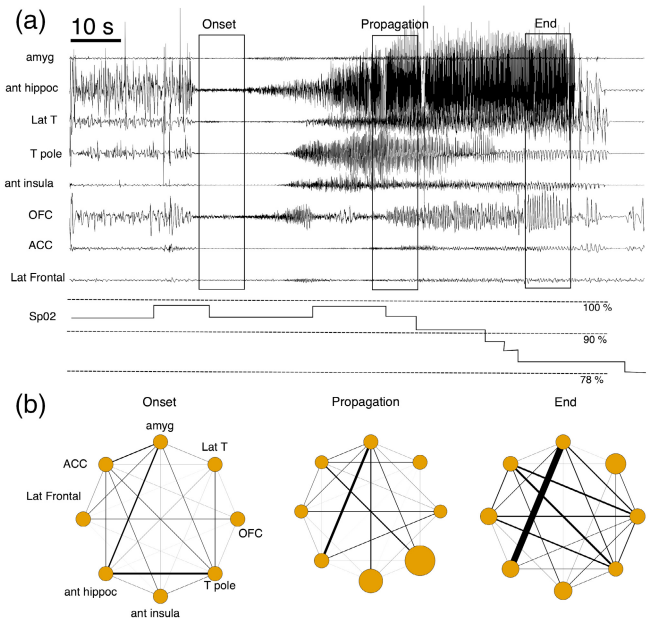

FIGURE 1 Example of SEEG signal analysis (ictal propagation and connectivity analysis) in one seizure with PIH (a) The panel shows raw SEEG signals recorded in a seizure of patient (P12) with PIH occurring during the propagation of the seizure. Signals recorded in eight regions of interest are shown: ACC, anterior cingulate cortex; amyg, amygdala; ant hippoc, anterior hippocampus; ant insula, anterior insula; Lat Frontal, lateral frontal cortex; Lat T. lateral temporal neocortex; OFC, orbito-frontal cortex; T Pole, temporal pole. (b) The panel shows the intensity of ictal propagation and functional connectivity for three periods (seizure onset, seizure propagation, seizure end) for the eight regions of interest. The size of the nodes is proportional to the [1–50 Hz] activity while the size of the edges is proportional to the [1–50 Hz] iCOH between the nodes.

2.3.3 | Quantitative analyses of SEEG data

For each seizure, several quantitative indices based on SEEG signal analysis were computed in order to investigate the following processes: i) epileptogenicity of the brain structures at seizure onset, ii) ictal propagation, and iii) network connectivity changes during seizures.

Epileptogenicity analysis

The epileptogenicity of each region of interest at seizure onset was investigated using the Epileptogenicity Index (EI) that inspired a number of studies aimed at identifying the epileptogenic zone from SEEG recording (Bartolomei et al., 2008) . EI combines the ratio of fast frequencies (beta/gamma) relative to slower frequencies and the time of involvement of each region. The EI is a normalized value that ranges from 0 (no epileptogenicity) to 1 (peak epileptogenicity) in the selected channels. The EI was calculated for all seizures within the subset of selected SEEG channels using the Anywave Software (available at https://meg.univ-amu.fr/wiki/AnyWave:Plugin_EI). In parallel, classical visual analysis of SEEG signals was checked by an SEEG expert (JJ) for each seizure: EI value was considered valid if bipolar contacts with high EI values (above 0.4) were congruent with seizure onset-zone determined with visual analysis.

Ictal propagation analysis

In order to evaluate the propagation of the discharge, we evaluated the strength of the ictal discharge during the seizure for each ROI. First, the bipolar SEEG signals were band-pass filtered in the [1–50 Hz] band. Subsequently a Hilbert transform of the filtered signals was performed. The power of the complex Hilbert transform was extracted for all time periods during the seizure (baseline, seizure onset, seizure propagation, and seizure end) and the activity for each of them was Z-score normalized relatively to the mean activity during the baseline, producing a Z-score normalized Ictal Propagation activity (IP: Ictal propagation). Because ictal hypoxemia typically persists after the end of the seizure, a similar analysis of the SEEG signal recorded over the first 10 s of the post-ictal period was also performed. In line with previous studies which reported that prolonged seizures leading to PIH are followed by a marked increase of slow wave activity or even suppression of neural activity that lasts several minutes

(Pottkämper et al., 2020; Yang et al., 2012), EEG activity [1–50 Hz] was strongly decreased in the post-ictal period with values approximating nullity in most of the regions of interest studied. Accordingly, the variance of the median values of post-ictal activity for each region of interest was almost null, precluding the use of linear models for robust statistical analysis. In this context, the post-ictal phase could not be included in further analyses. The ictal propagation was computed using the Brainstorm software (available at https://neuroimage.usc.edu/brainstorm/Introduction).

Network changes

In order to evaluate the changes of network connectivity associated with seizures, a functional connectivity (FC) analysis was performed. FC was evaluated with the Imaginary Part of Coherency (ICoh), capturing true neural interactions at a given time lag. (Nolte et al., 2004) The ICoh is a normalized value ranging between 0 (no interaction) to 1 (perfect synchrony between brain signals). The ICoh was computed using sliding windows of 4 s with 50% overlap. The ICoh in the [1–50 Hz] frequency band was computed pairwise between all regions for each time period. Focusing on a large frequency band of interest [1 50 Hz] allows to study interactions during the propagation and termination of the seizures, that are dominated by large frequency band neural activities. Bipolar contacts located in the orbito-frontal cortex, anterior cingulate, and lateral frontal cortex were pooled in the same subregion (frontal cortex).

2.3.4 | Pulse oximetry analysis

Pulse oximetry was recorded during the whole seizure using an Xpod pod oximeter (Nonin Medical Inc, Plymouth, MI, USA) connected to the video SEEG system.

Peri-ictal hypoxemia (PIH) was defined as SpO2 < 90% during at least 5 s occurring during the ictal period, the post-ictal period, or both.

The nadir of the SpO2, the time of onset of hypoxemia, and its total duration were also collected.

Subsequently, each period during the seizure (seizure onset, seizure propagation, and seizure end) was labeled as a PIH + period or PIH – period, depending on the presence of ongoing PIH during the period.

Figure 1 shows an example of SEEG signal analysis in one seizure with PIH.

2.4 | Statistical analyses

Association between occurrence of PIH and person- (age, gender, age of onset of epilepsy, presence of MRI epileptogenic lesion, epilepsy type, and surgical outcome) or seizure-specific (uni or bi-temporal propagation of ictal activity, seizure duration) variables was assessed with chi-square, or Wicoxon-Mann-Whitney *U* tests were appropriate. Comparisons between PIH latency and Nadir in patients with or without hippocampal sclerosis were performed using Wilcoxon-Mann-Whitney *U* tests. Correlations between descriptive parameters of PIH (duration, nadir, and time of onset) and seizure-specific variables (seizure duration, Epileptogenicity Index) was assessed using Spearman nonparametric correlation test.

For all those tests, the significance value was set at $p < .05$ corrected for multiple comparisons using False-Discovery-rate (FDR) procedure.

The main objective of SEEG statistical analyses was to test the hypotheses that epileptogenicity, ictal propagation, and connectivity depend on PIH occurrence and brain ROI. For those analyses, SEEG indices were considered as the response variable.

2.4.1 | Epileptogenicity analysis

To investigate this hypothesis, the relationship between epileptogenicity of brain structures and PIH was tested using a generalized linear model using a binomial error distribution. EI was considered as the variable to be explained while explicative variables were brain region and occurrence of PIH at the seizure level. Differences of EI between brain regions were evaluated with a nonparametric Wilcoxon test. All statistical tests were two-tailed and a p value of <.05 was chosen to indicate a significant result.

2.4.2 | Ictal propagation analysis

The relationship between ictal propagation (IP) and PIH was tested using a generalized linear mixed effect model. IP was considered as the variable to be explained while explicative variables were brain ROI, period of interest, and presence of PIH at each ictal period (fixed effects). Interactions between those factors were also modeled. Random effect was the subject. Post hoc tests were performed when needed to assess the differences between levels of significant variables with correction for multiple comparisons using the FDR procedure.

In order to evaluate the relationship between ictal propagation and the intensity of PIH, a secondary analysis was performed including only seizures with occurrence of PIH. For this analysis, a generalized linear mixed effect model was also used. IP was considered as the variable to be explained while explicative variables were ROI, period of interest, and nadir of PIH (fixed effects). To account for the nonlinearity of Nadir effect, a natural cubic spline with two degrees of freedom was used. Interactions between those factors were also modeled. Random effect was the subject. Post hoc tests were performed when needed to assess the differences between levels of significant variables with correction for multiple comparisons using the FDR procedure.

2.4.3 | Network changes

The relationship between functional connectivity and PIH was tested using a generalized linear mixed effect model. FC was considered as the variable to be explained while explicative variables were brain ROI,

period of interest, and occurrence of PIH during each ictal period (fixed effects). Interactions between those factors were also modeled. Random effect was the subject. Post hoc tests were performed when needed to assess the differences between levels of significant variables with correction for multiple comparisons using the FDR procedure.

All statistical analyses were performed using R.B using the R software (https://www.r-project.org) (version 4.0.3). GLMMs were fitted to the data using lme4 and the afex packages. Post hoc investigation of significant interactions was achieved using the framework provided by emmeans package. Supplementary information regarding the appropriateness and framework of generalized linear mixed effect model are provided in Appendix S1.

3 | RESULTS

3.1 | Characteristics of patients and seizures

In the present study, patients with focal epilepsy for whom ictal clinical features and scalp EEG suggested predominant involvement of temporal lobe structures but with atypical features for medial temporal lobe syndrome including i) atypical ictal symptoms (symptoms suggesting propagation to neocortical regions or insula or perisylvian cortex); ii) unusual ictal EEG pattern; and iii) absence of hippocampal sclerosis.

Among the 38 patients included in the study, 27 were males (71%). The mean age of patients was 37.8 ± 9.2 years (mean ± SD) and their mean age at epilepsy onset was 16.9 ± 9.2 years. Fifteen patients (53.6%) had hippocampal sclerosis on brain MRI. Twenty-six patients underwent surgical resection following SEEG: 13/26 (50%) had favorable outcome following surgery (Engel I class outcome with a minimum duration of follow-up of 1 year after surgery), while 13/26 (50%) had a bad outcome following surgery (Engel II, III, or IV class following surgery). Twelve patients were not operated upon: surgery was not performed either because of functional risk (risk of verbal memory decline for dominant hemisphere) or either because patient declined surgery.

A total of 40 seizures were included in the study. The mean seizure duration was 103.9 ± 80.4 s (range 13–422 s). As detailed in the methods section and in Table S2, SEEG electrodes primarily sampled the temporal lobe and perisylvian cortex, with bilateral exploration in 16 patients (42%). Clinical interpretation of SEEG seizures disclosed a late propagation of ictal activity in both temporal lobes during the course of the seizures in 10/16 seizures; however, seizure-onset zone was always considered unilateral and ictal discharge was systematically stronger in one temporal lobe.

3.2 | Relation between PIH and patients and/or seizure characteristics

PIH occurred in 20/40 seizures (50%). For the 20 seizures with PIH, the PIH started in average 59.2 s ± 40.4 after seizure onset. The mean duration of PIH was 78.2 s ± 41.2 (range 16–198). The mean Nadir of PIH was 82.7% ± 6.2. The onset time of PIH was at seizure onset for 10% of the seizures, during seizure propagation for 40% of the seizures, at seizure end for 50% of the seizures. PIH was present at seizure onset for 10% of the seizures, during seizure propagation for 50% of the seizures, at seizure end for 70% of the seizures, and persisted during the post-ictal period for 90% of the seizures. Details on seizure characteristics, PIH characteristics (duration, onset latency, nadir) and cardiac changes are provided in Table S4. The mean onset latency and the mean Nadir of PIH were not different for patients with or without hippocampal sclerosis ($p > .05$).

No difference in mean age, sex ratio, age of onset of epilepsy, presence of hippocampal sclerosis, surgical outcome, and bilateral propagation to temporal lobes was evidenced when comparing seizures with PIH and seizures without PIH (Table 1).

Seizure duration was longer for seizures with PIH (120.5 s ± 88.4 sec) than seizures without PIH (87.3 s ± 70.9 sec, $p = .03$). There was no correlation between seizure duration and Nadir of PIH ($p > .05$), neither between seizure duration and duration of PIH ($p > .05$).

3.3 | Relation between PIH and Epileptogenicity of brain structures

EI was significantly dependent of brain ROI ($p < 1.10^{-9}$) but was independent of occurrence of PIH ($p > .05$), without significant interaction

TABLE 1 Comparison of the clinical characteristics of the patients for the seizures with and without PIH

	PIH ($n = 20$)	No PIH ($n = 20$)	Difference
Age (years)	40 (5.6)	34.7 (8.2)	NS
Sex ratio	0.75	0.7	NS
Epilepsy onset (years)	16 (6.2)	17.6 (3.8)	NS
HS	9 (45%)	6 (30%)	NS
Favorable surgical outcome	8 (47%)	5 (31%)	NS
Bilateral propagation	7/8 (87%)	3/8 (37%)	NS

Note: Age is expressed in mean age in years (SD); Epilepsy Onset is expressed in mean age of first seizure (SD); HS: Hippocampal Sclerosis shown is the number of patients with Hippocampal Sclerosis (proportion of patients); Favorable surgical outcome: number and proportion of patient with Engel 1 outcome; Bilateral propagation: number and proportion of patients with seizures that propagated in both temporal lobes during seizure evolution; Difference: NS: Nonsignificant.

between ROI and PIH. Post hoc analyses of the brain structure factor showed that EI was significantly higher for anterior hippocampus, amygdala, and temporal pole than the majority of other structures implanted (lateral temporal neocortex, frontal lateral cortex, orbito frontal cortex, and anterior cingulate). Anterior hippocampus had higher EI than temporal pole but not different from amygdala. The brain structure with highest EI was the hippocampus for 22 seizures (55%), the amygdala for five seizures (12.5%), in the temporal pole for five seizures (12.5%), in the insula for two seizures (5%), in the lateral temporal neocortex for one seizure (2.5%), and in other ROI for four seizures (10%).

For seizures with PIH, there was no correlation between EI and Nadir of PIH, neither between EI and duration of PIH. The main effect of ROI on EI is presented in Figure 2 and detailed results for EI are in Appendix S2.

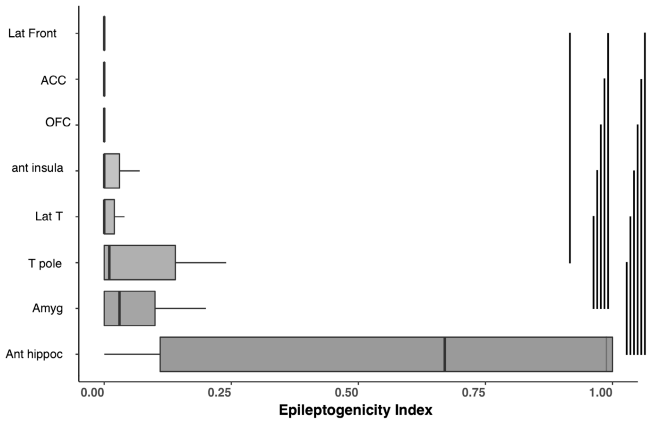

FIGURE 2 Epileptogenicity index of the regions of interest
Figure 2 shows the epileptogenicity of the regions of interests evaluated with the Epileptogenicity Index (EI). Bar plots show upper quartile, lower quartile, and median Significant EI differences between regions of interest are expressed with vertical bars on the right side of Figure (p < .05 nonparametric test). ACC, anterior cingulate cortex; ant hippoc, anterior hippocampus; ant insula, anterior insula; Lat Frontal, lateral frontal cortex; Lat T, lateral temporal neocortex; OFC, orbito-frontal cortex; T Pole, temporal pole.

3.4 | Relation between SEEG ictal propagation and occurrence of PIH

Linear mixed model analysis showed that ictal propagation was dependent on brain ROI factor ($p < 1.\ 10^{-4}$). A significant influence of interaction between brain ROI and period of interest, between brain ROI and occurrence of PIH and between brain ROI, period and occurrence of PIH (each factor $p < 1.\ 10^{-4}$) were also observed. Post hoc analyses showed that ictal propagation was stronger for some structures and for some periods when PIH occurred: i) during seizure propagation, ictal propagation in the [1–50 Hz] band was stronger in the amygdala and anterior insula, and ii) at seizure end, ictal propagation was stronger in amygdala, temporal lateral neocortex, anterior cingulate, anterior hippocampus, and temporal pole ($p < 1.\ 10^{-4}$). The comparison of ictal propagation according to PIH occurrence are presented in Figure 3 and detailed results for ictal propagation are in Appendix S2.

A secondary analysis focusing on seizures with PIH was performed to evaluate the relation between ictal propagation and Nadir of PIH (Figure 4 and Appendix S2 for detailed results). Ictal propagation was dependent on brain ROI and period of interest. A significant interaction was observed between brain ROI, period of interest and

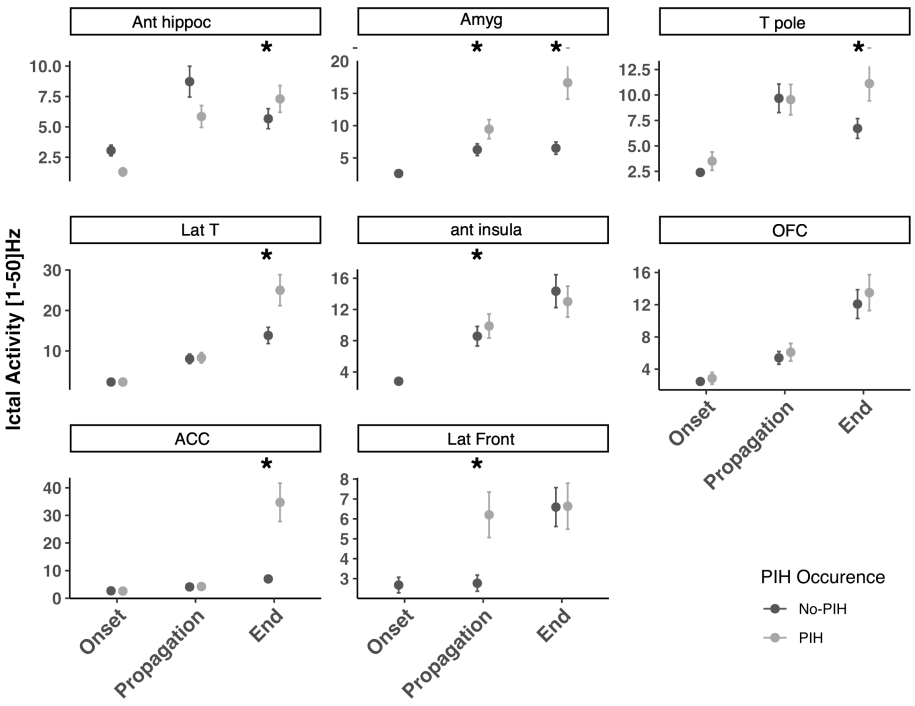

FIGURE 3 Ictal propagation for seizures with and without PIH occurrence
Figure 3 shows the ictal propagation expressed as [1–50 Hz] activity for the different regions of interests during the onset, propagation, and at the end of the seizures. Ictal propagation was evaluated for seizures with PIH and without PIH occurrence. Significant differences between seizures with PIH and without PIH occurrence are depicted with a star (post hoc tests with p value below .05, applied on linear mixed effect models after multiple comparisons correction). ACC, anterior cingulate cortex; ant hippoc: anterior hippocampus; ant insula: anterior insula; Lat Frontal, lateral frontal cortex; Lat T, lateral temporal neocortex; OFC, orbito-frontal cortex; T Pole: temporal pole

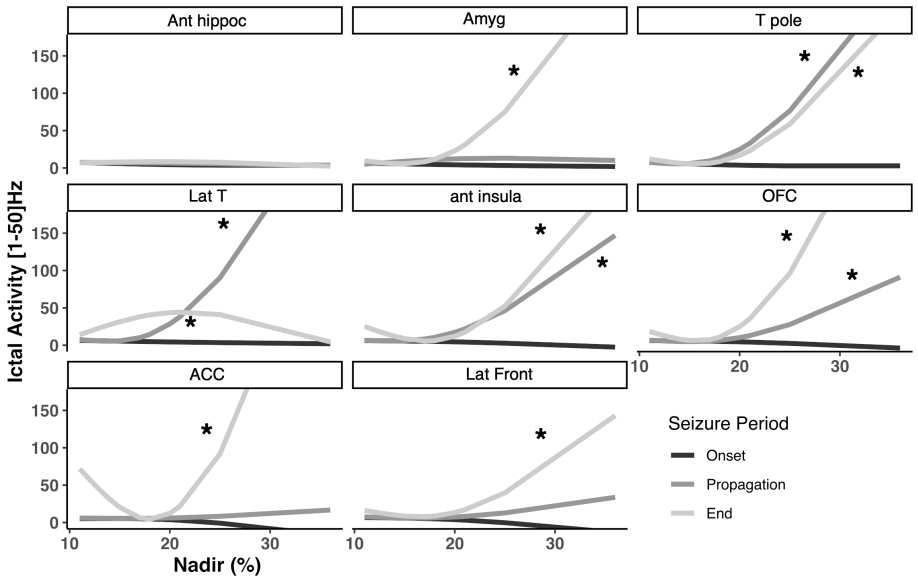

FIGURE 4 Relationship between ictal propagation and intensity of PIH Figure 4 shows the relationship between ictal propagation expressed as [1–50 Hz] activity and intensity of PIH (expressed as 100 minus the Nadir of SaO2 in percentage) for the regions of interest. Significant statistical relations between Ictal Propagation and intensity of PIH for each seizure period are depicted with a star (post hoc tests with *p* value below .05, applied on linear mixed effect models after multiple comparisons correction). ACC, anterior cingulate cortex; ant hippoc, anterior hippocampus; ant insula: anterior insula; Lat Frontal: lateral frontal cortex; Lat T, lateral temporal neocortex; OFC, orbito-frontal cortex; T Pole, temporal pole;

Nadir of PIH ($p < 1.\ 10^{-4}$). Post hoc analyses showed that ictal propagation was correlated with the Nadir of PIH i) in the propagation period for anterior insula, temporal lateral neocortex, temporal pole and ii) at the end of seizure for anterior insula, orbitofrontal cortex, temporal lateral neocortex, amygdala, anterior cingulate, and temporal pole.

Lastly, for seizures with PIH, no significant relation was observed between duration of PIH and ictal propagation.

3.5 | Relation between ictal network connectivity and occurrence of PIH

Network connectivity analyses showed that functional connectivity in the [1–50 Hz] band between brain ROI was dependent on brain ROI and interaction between periods of interest and occurrence of PIH ($p < 1.\ 10^{-4}$). Post hoc analyses focusing on brain ROI showed that the connectivity between amygdala and anterior hippocampus was higher than the majority of connections between other brain structures ($p < 1.\ 10^{-4}$). Post hoc analyses focusing on the interaction between periods of interest and occurrence of PIH showed that an overall higher functional connectivity between brain structures in the propagation period ($p < 1.\ 10^{-4}$).

Those results are presented in Figure 5 and Appendix S2.

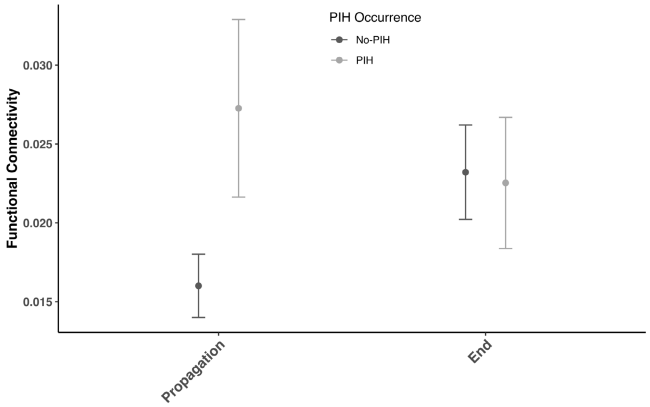

FIGURE 5 Functional connectivity changes for seizures leading to PIH Figure 5 shows the mean functional connectivity (iCOH in the [1–50 Hz] band) between regions of interest during the propagation and at the end of the seizures. Linear mixed effect model analysis showed that mean functional connectivity was higher during the propagation period for seizures leading to PIH (post hoc tests with *p* value below .05 corrected for multiple comparisons). The structure variable of the linear mixed effect was not significant, suggesting that the increase of connectivity was not specific to individual brain regions of interest.

4 | DISCUSSION

In the present study, we demonstrated that the occurrence of ictal hypoxemia in seizures originating from the temporal lobe is associated with an intense propagation to several key regions within temporal lobe, insula and frontal cortex and higher functional connectivity between those structures. Seizures with longer duration were at greater risk of PIH, in line with several previous studies. (Barba et al., 2016; Bateman et al., 2008) In contrast, seizure duration was not correlated with the intensity of PIH. This finding contradicted results from Bateman et al. who found that the duration of focal seizures was correlated with intensity of PIH (Bateman et al., 2008). However, seizures were recorded with scalp video EEG in that study, blurring precise estimation of seizure start and ending. Most importantly, our study suggests that seizure duration is not by itself a major determinant factor of PIH. Seizure propagation pathways were more closely related to intensity of PIH than overall seizure duration.

At seizure onset, most of the seizures disclosed the highest epileptogenicity in medial temporal lobe structures (amygdala, hippocampus) or temporal pole. However, there was no association between

epileptogenicity of those structures and PIH occurrence. Only very few intracranial EEG studies reported spontaneous seizures leading to ictal apnea and/or PIH. Those studies suggested a key role of the medial temporal structures at seizure onset (Lacuey, Hampson, et al., 2019; Lacuey, Hupp, et al., 2019; Nobis et al., 2019) but the relative epileptogenicity of those structures was not quantified. Our study suggests that the localization value of PIH for the determination of the structure with highest epileptogenicity (between hippocampus, amygdala and temporal pole) at seizure onset is limited. Anterior insula was not associated with occurrence of PIH at seizure onset; however, very few seizures originated from insula and the role of this region may be evaluated in following studies focusing directly on insular epilepsy.

In contrast, seizure spread was different for seizures with PIH and seizures without PIH, with stronger propagation to amygdala and anterior insula during the middle part of the seizure when PIH occurred. It is well established that electrical stimulation of the amygdala reliably induces central apnea. Amygdala could be a key node of a limbic/paralimbic mesial temporal breathing modulation network including amygdala, hippocampus, anterior parahippocampal, and antero-mesial fusiform gyri (Lacuey, Hampson, et al., 2019). Our study also highlights the role of anterior insula, in accordance with several reports showing the role of this region in breathing modulation. (Frysinger & Harper, 1989; Hoffman & Rasmussen, 1953; Kaada & Jasper, 1952b; Loizon et al., 2020; Penfield & Faulk, 1955) However, our study is the first to show a direct link between seizure spread within the insula and PIH occurrence during spontaneous seizures. At the end of the seizures, PIH occurrence was associated with a more widespread involvement including amygdala, anterior hippocampus, temporal pole, anterior cingulate, and temporal lateral neocortex. Several earlier studies showed that those structures have direct or indirect projections to brainstem respiratory centers and that their electrical stimulation can induce apnea (Lacuey, Hampson, et al., 2019; Loizon et al., 2020).

The intensity of PIH was correlated with implication of several structures during seizure propagation including anterior insula, temporal pole and temporal lateral neocortex, and at seizure end (anterior insula, amygdala, anterior cingulate, orbitofrontal cortex, temporal pole, and temporal lateral neocortex). Those results suggested that PIH occurrence and PIH intensity are not governed by the same neural mechanisms. While anterior insula, amygdala and temporal pole activations are both related to PIH occurrence, activations within temporal lateral neocortex, anterior cingulate, and orbito frontal cortex might reflect more indirect phenomena related to overall seizure spread.

We also showed here that seizures leading to PIH were characterized by a higher functional connectivity between regions of interest during ictal propagation period, but not at the termination of the seizure. We found a global increase of connectivity between medial temporal lobe, temporal pole, insula, and lateral temporal neocortex during propagation. As a whole, this suggests that PIH emergence is related to the activation of a large network involving the medial temporal lobe, anterior insula, lateral temporal neocortex, and frontal structures. These observations argue against the hypothesis of a strictly focal focus generating PIH. It is well known that several cortical structures contribute to respiratory control (Binks et al., 2014; Evans, 2010) and changes of global synchrony within that widespread network may be necessary to trigger PIH. As such, amygdala and anterior insula may be considered as key nodes within that network but their stronger activation does not resume the whole story. From a clinical perspective, this suggests that PIH occurrence during temporal lobe seizures is not fully explained by a strictly focal involvement of amygdala or insula.

Several limitations of our study need to be considered. According to our inclusion criteria, we investigated seizures originating mostly from medial temporal lobe structures. Although insula, lateral temporal structures and frontal lobe were sampled in the majority of the patients, investigating the relation between PIH and the involvement of these structures at seizure onset will require a dedicated study. Moreover, the role of some subcortical structures involved in respiratory control (such as hypothalamus or basal ganglia (Macey et al., 2015)) cannot be assessed by SEEG recordings. Secondly, the respiratory monitoring in patients included in our study was restricted to SpO_2. In the absence of plethysmography, we could not confirm directly that the SpO_2 decrease resulted from central apnea. Studying respiratory activity with respiratory belts would allow to evaluate directly the link between ictal activity and apnea. However, several previous studies showed that ictal hypoxemia in focal seizures is accompanied by central apnea, assessed either by direct measures of respiratory function with respiratory belts or by the simultaneous use of ETCO2 measurement (an index of hypoventilation), supporting a centrally mediated ventilatory dysfunction. (Bateman et al., 2008; Seyal et al., 2010; Singh et al., 2013)

In conclusion, the present study shows that focal temporal lobe seizures leading to PIH are associated with strong propagation to amygdala and anterior insula during seizure spread and a more widespread increase of synchrony between brain structures involved in respiratory control. Those results suggest that PIH occurrence during temporal lobe seizures may be related to the activation of a widespread network of cortical structures, among which amygdala and anterior insula are key nodes.

STANDARD PROTOCOL APPROVALS, REGISTRATION AND PATIENT CONSENTS

The $REPO_2MSE$ study has been approved by the ethics committee (CPP Sud Est II n°2010-006-AM6) and competent authority (ANSM n° B100108-40). All patients gave written informed consent.

ACKNOWLEDGMENTS

The $REPO_2MSE$ study was funded by the French Ministry Of Health (PHRC National 2011).

CONFLICT OF INTEREST

None of the authors has any conflict of interest to disclose. We confirm that we have read the Journal's position on issues involved in ethical publication and affirm that this report is consistent with those guidelines.

DATA AVAILABILITY STATEMENT

The data used in this study are available from the corresponding author upon reasonable request.

ORCID

Julien Jung https://orcid.org/0000-0002-9274-0086
Sylvain Rheims https://orcid.org/0000-0002-4663-8515

REFERENCES

Barba, C., Rheims, S., Minotti, L., Guénot, M., Hoffmann, D., Chabardès, S., Isnard, J., Kahane, P., & Ryvlin, P. (2016). Temporal plus epilepsy is a major determinant of temporal lobe surgery failures. *Brain*, *139*(Pt 2), 444–451.

Bartolomei, F., Chauvel, P., & Wendling, F. (2008). Epileptogenicity of brain structures in human temporal lobe epilepsy: A quantified study from intracerebral EEG. *Brain*, *131*(Pt 7), 1818–1830.

Bartolomei, F., Wendling, F., Bellanger, J. J., Régis, J., & Chauvel, P. (2001). Neural networks involving the medial temporal structures in temporal lobe epilepsy. *Clinical Neurophysiology*, *112*(9), 1746–1760.

Bateman, L. M., Li, C.-S., & Seyal, M. (2008). Ictal hypoxemia in localization-related epilepsy: Analysis of incidence, severity and risk factors. *Brain*, *131*(Pt 12), 3239–3245.

Binks, A. P., Evans, K. C., Reed, J. D., Moosavi, S. H., & Banzett, R. B. (2014). The time-course of cortico-limbic neural responses to air hunger. *Respiratory Physiology & Neurobiology*, *204*, 78–85.

Dlouhy, B. J., Gehlbach, B. K., Kreple, C. J., Kawasaki, H., Oya, H., Buzza, C., Granner, M. A., Welsh, M. J., Howard, M. A., Wemmie, J. A., & Richerson, G. B. (2015). Breathing inhibited when seizures spread to the amygdala and upon amygdala stimulation. *The Journal of Neuroscience*, *35*(28), 10281–10289.

Evans, K. C. (2010). Cortico-limbic circuitry and the airways: Insights from functional neuroimaging of respiratory afferents and efferents. *Biological Psychology*, *84*(1), 13–25.

Frysinger, R. C., & Harper, R. M. (1989). Cardiac and respiratory correlations with unit discharge in human amygdala and hippocampus. *Electroencephalography and Clinical Neurophysiology*, *72*(6), 463–470.

Hoffman, B. L., & Rasmussen, T. (1953). Stimulation studies of insular cortex of Macaca mulatta. *Journal of Neurophysiology*, *16*(4), 343–351.

Kaada, B. R., & Jasper, H. (1952a). Respiratory responses to stimulation of temporal pole, insula, and hippocampal and limbic gyri in man. *A.M.A. Archives of Neurology and Psychiatry*, *68*(5), 609–619.

Lacuey, N., Hampson, J. P., Harper, R. M., Miller, J. P., & Lhatoo, S. (2019). Limbic and paralimbic structures driving ictal central apnea. *Neurology*, *92*(7), e655–e669.

Lacuey, N., Hupp, N. J., Hampson, J., & Lhatoo, S. (2019). Ictal central apnea (ICA) may be a useful semiological sign in invasive epilepsy surgery evaluations. *Epilepsy Research*, *156*, 106164.

Lacuey, N., Zonjy, B., Hampson, J. P., Rani, M. R. S., Zaremba, A., Sainju, R. K., Gehlbach, B. K., Schuele, S., Friedman, D., Devinsky, O., Nei, M., Harper, R. M., Allen, L., Diehl, B., Millichap, J. J., Bateman, L., Granner, M. A., Dragon, D. N., Richerson, G. B., & Lhatoo, S. D. (2018). The incidence and significance of periictal apnea in epileptic seizures. *Epilepsia*, *59*(3), 573–582.

Lacuey, N., Zonjy, B., Londono, L., & Lhatoo, S. D. (2017). Amygdala and hippocampus are symptomatogenic zones for central apneic seizures. *Neurology*, *88*(7), 701–705.

Loizon, M., Ryvlin, P., Chatard, B., Jung, J., Bouet, R., Guenot, M., Mazzola, L., Bezin, L., & Rheims, S. (2020). Transient hypoxemia induced by cortical electrical stimulation: A mapping study in 75 patients. *Neurology*, *94*(22), e2323–e2336.

Macey, P. M., Ogren, J. A., Kumar, R., & Harper, R. M. (2015). Functional imaging of autonomic regulation: Methods and key findings. *Frontiers in Neuroscience*, *9*, 513.

Maillard, L., Vignal, J.-P., Gavaret, M., Guye, M., Biraben, A., McGonigal, A., Chauvel, P., & Bartolomei, F. (2004). Semiologic and electrophysiologic correlations in temporal lobe seizure subtypes. *Epilepsia*, *45*(12), 1590–1599.

Nobis, W. P., González Otárula, K. A., Templer, J. W., Gerard, E. E., VanHaerents, S., Lane, G., Zhou, G., Rosenow, J. M., Zelano, C., & Schuele, S. (2019). The effect of seizure spread to the amygdala on respiration and onset of ictal central apnea. *Journal of Neurosurgery*, *132*(5), 1313–1323.

Nolte, G., Bai, O., Wheaton, L., Mari, Z., Vorbach, S., & Hallett, M. (2004). Identifying true brain interaction from EEG data using the imaginary part of coherency. *Clinical Neurophysiology*, *115*(10), 2292–2307.

Ochoa-Urrea, M., Dayyani, M., Sadeghirad, B., Tandon, N., Lacuey, N., & Lhatoo, S. D. (2021). Electrical Stimulation-Induced Seizures and Breathing Dysfunction: A Systematic Review of New Insights Into the Epileptogenic and Symptomatogenic Zones. *Frontiers in Human Neuroscience*, *14*, 617061.

Park, K., Kanth, K., Bajwa, S., Girgis, F., Shahlaie, K., & Seyal, M. (2020). Seizure-related apneas have an inconsistent linkage to amygdala seizure spread. *Epilepsia*, *61*(6), 1253–1260.

Penfield, W., & Faulk, M. E. (1955). The insula; further observations on its function. *Brain*, *78*(4), 445–470.

Pottkämper, J. C. M., Hofmeijer, J., van Waarde, J. A., & van Putten, M. J. A. M. (2020). The postictal state - what do we know? *Epilepsia*, *61*(6), 1045–1061.

Ryvlin, P., Nashef, L., Lhatoo, S. D., Bateman, L. M., Bird, J., Bleasel, A., Boon, P., Crespel, A., Dworetzky, B. A., Høgenhaven, H., Lerche, H., Maillard, L., Malter, M. P., Marchal, C., Murthy, J. M. K., Nitsche, M., Pataraia, E., Rabben, T., Rheims, S., … Tomson, T. (2013). Incidence and mechanisms of cardiorespiratory arrests in epilepsy monitoring units (MORTEMUS): A retrospective study. *Lancet Neurology*, *12*(10), 966–977.

Seyal, M., Bateman, L. M., Albertson, T. E., Lin, T.-C., & Li, C.-S. (2010). Respiratory changes with seizures in localization-related epilepsy: Analysis of periictal hypercapnia and airflow patterns. *Epilepsia*, *51*(8), 1359–1364.

Singh, K., Katz, E. S., Zarowski, M., Loddenkemper, T., Llewellyn, N., Manganaro, S., Gregas, M., Pavlova, M., & Kothare, S. V. (2013). Cardiopulmonary complications during pediatric seizures: A prelude to understanding SUDEP. *Epilepsia*, *54*(6), 1083–1091.

Tio, E., Culler, G. W., Bachman, E. M., & Schuele, S. (2020). Ictal central apneas in temporal lobe epilepsies. *Epilepsy & Behavior*, *112*, 107434.

Vilella, L., Lacuey, N., Hampson, J. P., Rani, M. R. S., Loparo, K., Sainju, R. K., Friedman, D., Nei, M., Strohl, K., Allen, L., Scott, C., Gehlbach, B. K., Zonjy, B., Hupp, N. J., Zaremba, A., Shafiabadi, N., Zhao, X., Reick-Mitrisin, V., Schuele, S., … Lhatoo, S. D. (2019). Incidence, recurrence, and risk factors for Peri-ictal central apnea and sudden unexpected death in epilepsy. *Frontiers in Neurology*, *10*, 166.

Yang, L., Worrell, G. A., Nelson, C., Brinkmann, B., & He, B. (2012). Spectral and spatial shifts of post-ictal slow waves in temporal lobe seizures. *Brain*, *135*(Pt 10), 3134–3143.

SUPPORTING INFORMATION

Additional supporting information can be found online in the Supporting Information section at the end of this article.

How to cite this article: Jung, J., Bouet, R., Catenoix, H., Montavont, A., Isnard, J., Boulogne, S., Guénot, M., Ryvlin, P., & Rheims, S. (2022). Peri-ictal hypoxemia during temporal lobe seizures: A SEEG study. *Human Brain Mapping*, *43*(15), 4580–4588. https://doi.org/10.1002/hbm.25975